Contactless measurement of short-range electron motion in semiconducting macroporous GaP

A. Germeau, E. van Faassen, and D. Vanmaekelbergh
Debye Institute, Utrecht University, P.O. Box 80000, 3508 TA Utrecht, The Netherlands
(Received 27 November 2001; published 10 April 2002)

Studies of long-range electron transport in porous semiconductors have shown that the effective mobility is strongly reduced with respect to that of single-crystalline bulk semiconductors. This strong attenuation of electron transport has been attributed to multiple trapping/detrapping in states located at the internal surface of the porous solid. Here we report microwave reflectivity measurements on a dark and illuminated macroporous GaP network which allow us to probe the trap-free mobility of electrons present inside the core of the network. We obtain the imaginary and real components of the dielectric constant, and the changes of these variables as a function of the incident light intensity. We show that the changes in the real and imaginary parts of the dielectric constant as a function of the light intensity are correlated, and can be interpreted on the basis of a hydrodynamic model. We find that the short-range electron mobility is 3 $cm^2/V\,s$. We compare this value with the mobility obtained from Hall-measurements on single crystals and the effective mobility characterizing long-range transport through a porous GaP network. The transient changes in the dielectric constant upon switching the light on and off reflect the dynamics of electron-hole photogeneration and bulk and surface recombination in the porous GaP network.

DOI: 10.1103/PhysRevB.65.165331 PACS number(s): 73.23.−b, 73.40.−c, 73.20.−r

INTRODUCTION

Porous semiconductors, which consist of electrically connected (nanometer-sized) crystals or of a single-crystalline network, have attracted much interest in the last decade.[1] These systems show promising properties for application in batteries (photoelectrochemical), solar cells,[2,3] electrochromic windows,[4,5] light-emitting diodes,[6] and photonic devices. In addition, porous semiconductors offer a set of challenging fundamental questions dealing with the short- and long-range transport of electrons and holes, and their recombination dynamics. Electron transport in porous semiconductors, such as TiO_2, ZnO, and GaP, was studied by a number of methods that measure the response of a photoelectrochemical device to a small-amplitude modulation of the absorbed light intensity.[7–14] Measurements on classic metal/semiconductor/metal systems were also performed.[15] In the case of macroporous GaP and microporous TiO_2 electrodes, it was shown that the transport-characteristics are nondispersive (Gaussian or normal); this means that all the photogenerated electrons behave in a similar way, and can be described by mean transport parameters.[16] One can thus use an effective mobility (often called the drift mobility) to quantify the long-range electron motion.[11,13,17,18] Nonetheless, long-range electron transport in porous semiconductors is strongly attenuated: the measured effective mobilities are 2–5 orders of magnitude smaller than those reported for the nonporous single crystalline counterparts (obtained from Hall conductivity measurements). This was attributed to multiple trapping or detrapping in localized energy levels located at the huge internal surface of the porous matrix. It has proven very difficult, however, to quantify the contribution of surface trapping in long-range transport by independent methods. In this respect, it would be of interest to measure the trap-free conduction mobility μ of electrons in a *porous semiconductor*.

In this paper we investigate the short-range motion of electrons in macroporous GaP by measurement of the interaction with microwaves. The motivation for this work is twofold. The main interest of this work can be appreciated by examining Figs. 1 and 2. Figure 1 shows a scanning electron micrograph (SEM) of the porous GaP that we used. Figure 2(a) sketches the energetics in the structural units under the given conditions; macroporous GaP can be mimicked by spheres (radius 75 nm), which consist of a *semiconducting* core (the radius denoted as R_c, electron density $n=3\times10^{17}$ cm^{-3}), surrounded by a region depleted of electrons. The depleted shell is due to the trapping of free electrons in surface states of energy in the band gap (the precise dimensions of both regions will be considered below). Figure 2(b) shows the penetration of the microwave electric field E in the structural units of this matrix, calculated with a hydrodynamic model discussed below. The field penetration according to the Mie model is also shown for comparison. It can be seen that the microwave field penetrates the *semiconducting* cores to a depth equal to the Debye screening length L, which here is close to 6 nm. The distance that an electron can migrate during one period of the microwave $2\pi/\omega$ is equal or less than $\mu E 2\pi/\omega$, which is about 1 nm. Thus the micro-

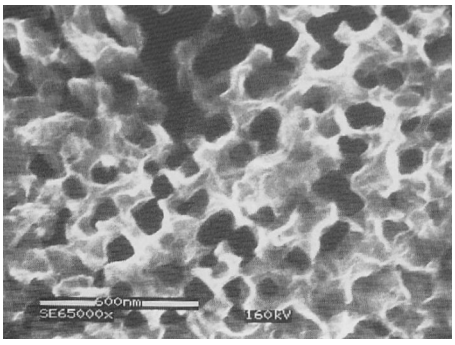

FIG. 1. SEM micrograph of anodic etched porous GaP. Dark areas indicate the absence of GaP material.

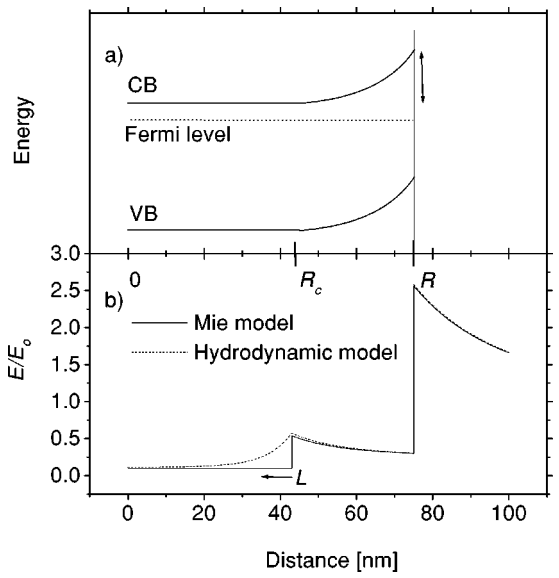

FIG. 2. (a) Schematic drawing of the edges of the conduction band (CB) and valence band (VB) with respect to the Fermi level for macroporous GaP (the band gap is 2.3 eV). The band bending ($\simeq$0.3 eV) is indicated with an arrow. A GaP sphere is used as a model; the sphere has an outer radius R of 75 nm, and consists of a semiconducting core with a radius R_c surrounded by a depletion layer. (b) The amplitude of the microwave-induced electric field in the nanoparticle relative to the amplitude of the applied microwave electric field is shown as a function of the distance in the direction of the applied field. In the hydrodynamic model the screening of the electric field in the conducting part occurs on a length scale of the Debye screening length L (=6.3 nm). In the Mie model the electric field changes discontinuously at the interface of the conducting and depleted regions. Outside the particle, the electric field falls off due to the induced dipole.

waves probe the electrons residing at the interface between the semiconducting core and the depleted region. These electrons are sufficiently remote from the surface; measurement of the short-range electron motion by microwave reflection should, therefore, provide the ''bulk'' mobility of the electrons in the porous matrix, free from the effects of surface trapping. This work is thus complementary to methods that measure the long-range transport parameters which are determined by surface trapping or detrapping.

A second motivation for this work is related to the interpretation of the results obtained with illuminated nanostructured semiconductors, probed with the (time-resolved) microwave conductivity method. The pioneering works of Deri and Spoonhower[19] and Grabtchak and Cocivera[20] on polycrystalline semiconductors (AgCl and CdSe) showed that the microwave absorption and the shift of the cavity resonance frequency provide the changes in the imaginary ($\Delta\epsilon''$) and real ($\Delta\epsilon'$) components of the dielectric constant due to photoexcitation of the nanostructured semiconductor. Interpretation of $\Delta\epsilon'$ and $\Delta\epsilon''$ is, however, less straightforward. References 19 and 20 attributed $\Delta\epsilon''$ to microwave absorption by photogenerated *free* carriers, while $\Delta\epsilon'$ was believed to correspond to *trapped* carriers. The observations that the decay of $\Delta\epsilon'$ and $\Delta\epsilon''$ transients show the same time constants, and showed that $\Delta\epsilon'$ and $\Delta\epsilon''$ depend in the same way on the intensity of photogeneration were attributed to fast equilibration between trapped and free charge carriers. Recently, one of us proposed a hydrodynamic model that considers the polarizability of an assembly of semiconducting spheres.[21] This model showed that photogeneration of excess free carriers in such a system leads to an increase of both $\Delta\epsilon''$ and $\Delta\epsilon'$; it thus provides a natural explanation for the previously reported correlation between $\Delta\epsilon''$ and $\Delta\epsilon'$. In the Appendix this hydrodynamic model is extended and adapted to the case of semiconducting spheres surrounded by a dielectric shell. The experimental results that we present can be understood quantitatively by this model. In Sec. III it will be shown that $\Delta\epsilon''$ and $\Delta\epsilon'$ correspond to the expansion of the semiconducting regions in the porous matrix due to the photogeneration of excess free electrons, and we discuss how we obtain from these quantities a value for the mobility μ inside the semiconducting part and the radius of the semiconducting part R_c. In Sec. IV, interpretations of $\Delta\epsilon'$ *and* $\Delta\epsilon''$ measured under steady-state conditions as a function of the incident light intensity, and of the transients $\Delta\epsilon'$ and $\Delta\epsilon''$ upon turning photoexcitation on and off provide interesting information on the electron-hole recombination dynamics in porous semiconductors.

EXPERIMENT

Single crystalline *n*-type GaP is made porous by anodic etching in a sulfunic acid solution. Afterward, the porosity of the anodically etched GaP is further increased from 25% to 50% by photoanodic etching in a H_2O:H_2SO_4:H_2O_2 electrolyte using 1.96-eV subband gap light.[22]

Scanning electron microscopy analysis (Fig. 1) reveals that we obtain a randomly porous matrix.[23,24] The GaP structures in this network have a typical length scale of about 150 nm. X-ray-diffraction measurements show that the semiconducting part in the porous structure is single crystalline.[23] For the microwave measurements 5 mg of porous material is scraped off the porous GaP electrode and compressed in a quartz capillary. The filling factor f of GaP in the capillary is 0.4. The dielectric constant of porous GaP is obtained from the measurement of the microwave reflection spectrum at a cavity loaded with the capillary. The microwave cavity consists of an *X*-band waveguide terminated at one side by a metal grid through which optical access is possible. The other end consists of a height-adjustable metal pin which only partially reflects the microwaves. The microwave power reflected at this cavity is amplified, down-converted in a detector, and displayed on an oscilloscope. By changing the height of the metal pin, we can reduce the reflection at the resonance frequency. In this way a large amplification can be achieved and the reflection spectrum can be measured very accurately. The reflection spectrum is only slightly perturbed by loading the cavity with a dielectric with a volume much smaller than the volume of the cavity and with a complex dielectric constant with a modulus close to 1. The decrease of the resonance frequency is then proportional to the real part of the dielectric constant ϵ', the increase of the width of the spectrum is proportional to the complex part of the di-

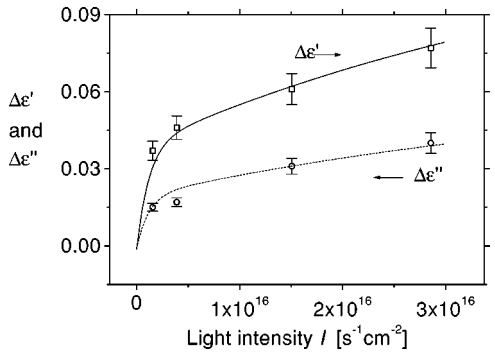

FIG. 3. The change in the complex dielectric constant of porous GaP $\Delta\epsilon$ as a function of the incident photon flux I. The experimental values for $\Delta\epsilon'$ and $\Delta\epsilon''$ are depicted as (□) and (○), respectively. These values are fitted with the hydrodynamic model by choosing the mobility $\mu=3$ cm^2/V s and the radius of the semiconducting part in the dark R_c $(P\text{dark})=45$ nm. The procedure is discussed in the text.

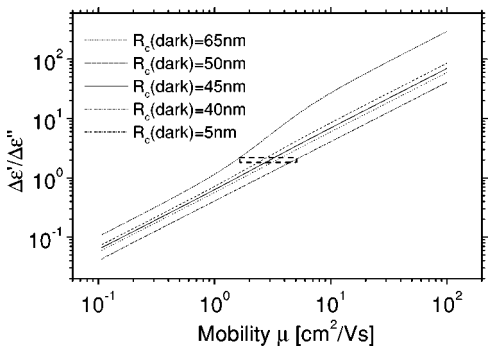

FIG. 4. The ratio $\Delta\epsilon'(I)/\Delta\epsilon''(I)$, calculated with the hydrodynamic model, is shown as a function of the mobility μ of free electrons in the semiconducting core, for different values of the radius of the semiconducting core R_c. The change in the dielectric constant is calculated as $\Delta\epsilon(I)=\epsilon[R_c(I)]-\epsilon[R_c(\text{dark})]$, with $R_c(I)-R_c=5$ nm. With an experimental value $\Delta\epsilon'/\Delta\epsilon''=2.0\pm0.1$, we conclude that the mobility lies between 1 and 5 cm^2/V s. (Only the lines that pass through the rectangle are compatible with the experimental value $\Delta\epsilon'/\Delta\epsilon''=2.0\pm0.1$.)

electric constant ϵ''.[25] A quantitative description of the change of the reflected spectrum as a function of the dielectric constant is calculated with the transmission line model.[26]

Porous GaP was illuminated in the cavity with a halogen lamp equipped with a filter transparant between 400 and 600 nm. Changes in ϵ' and ϵ'' were measured as a function of the incident light intensity (see Fig. 3). In addition the transient changes of ϵ' and ϵ'' upon turning the light on and off were recorded (see Fig. 8). Heating of the sample by the illumination causes an increase of the temperature of less than 10^{-2} K, which corresponds to changes in the dielectric constant two orders of magnitude smaller than the values we obtained. All measurements are performed at room temperature in contact with air.

DETERMINATION OF THE SHORT-RANGE MOBILITY IN MACROPOROUS GAP

The dielectric constant of porous GaP in the dark obtained from the microwave measurements (at a frequency of 8 GHz) is $\epsilon'+i\epsilon''=2.57\pm0.15+i0.07\pm0.05$. In effective-medium theory the dielectric constant of a mixture of air with a crystal with volume fraction f is given by $\epsilon=(1-f)+f\epsilon_{crystal}$. In this expression $\epsilon_{crystal}$ is the effective dielectric constant of crystalline GaP, which is the sum of the contributions from the bound electrons $\epsilon_b(=8.5)$ (Ref. 30) and the free electrons, described by a Drude term $i\sigma/\omega$. The conductivity of the free electrons at a radial frequency ω is denoted by σ. For our doped crystalline GaP $\epsilon_{crystal}=8.5+i1122.0$. With the independently determined value for f $(=0.4)$ we then obtain $\epsilon=4.0+i448.8$. This approximation thus overestimates the imaginary part of porous GaP by several orders of magnitude. In the Appendix a more realistic model is developed which takes into account surface polarization at the GaP spheres.

Figure 3 shows the changes in the dielectric constant of porous GaP under illumination as a function of the incident light intensity. The change in the real part of the dielectric constant $\Delta\epsilon'$ is of the same order and has the same sign as the imaginary part $\Delta\epsilon''$. The ratio $\Delta\epsilon'(I)/\Delta\epsilon''(I)$ is constant for all light intensities used in our experiments, and has a value $\Delta\epsilon'/\Delta\epsilon''=2.0\pm0.1$. We remark that the same ratio is found in time-resolved measurements (see Fig. 8). The experimental accuracy in $\Delta\epsilon'/\Delta\epsilon''$ is good because one needs to measure only small perturbations in ϵ and only the *ratio* of the real and imaginary part is involved.

Note that in effective medium theory with a conductivity given by $\sigma=[ne^2\tau/m(1-i\omega\tau)]$ (e is the elementary charge, m the effective mass of the charge carrier, τ the momentum ralaxation time, and n the density), an increase in the charge carrier density corresponds to a ratio $\Delta\epsilon'/\Delta\epsilon''=-\omega\tau$. In our experiments this would correspond to a negative ratio $\Delta\epsilon'/\Delta\epsilon''=-10^{-5}$, which is five orders of magnitude smaller than the experimental value.

In the Appendix we calculate the dielectric constant ϵ of a collection of semiconducting spheres of GaP (radius R_c) surrounded by a shell of (dielectric) GaP, depleted of free electrons. This calculation is an extension of the hydrodynamic model that was previously presented.[21] This model shows that the increase of $\Delta\epsilon'(I)$ and $\Delta\epsilon''(I)$ is due to the increase in the radius R_c of the semiconducting spheres in the GaP matrix with increasing light intensity I. A fit of $\Delta\epsilon'(I)$, $\Delta\epsilon''(I)$ by this model is presented by the solid lines in Fig. 3 (details are given below).

In Fig. 4 we plot the ratio $\Delta\epsilon'/\Delta\epsilon''$, calculated with the hydrodynamic model, as a function of the mobility μ, for different values of the radius $R_c(\text{dark})$ of the semiconducting part in the dark. The change in the dielectric constant is calculated as $\Delta\epsilon(I)=\epsilon[R_c(I)]-\epsilon[R_c(\text{dark})]$, assuming $R_c(I)-R_c(\text{dark})=5$ nm, a realistic change as can be seen below. From Fig. 4 we conclude that with an experimental value $\Delta\epsilon'/\Delta\epsilon''=2.0\pm0.1$ the mobility μ must lie between 1 and 5 cm^2/V s for all reasonable values for $R_c(\text{dark})$ $[0\leqslant R_c(\text{dark})\leqslant R]$. No information about the radius $R_c(\text{dark})$ is obtained from this plot.

In Fig. 5 we show the real part of the dielectric constant

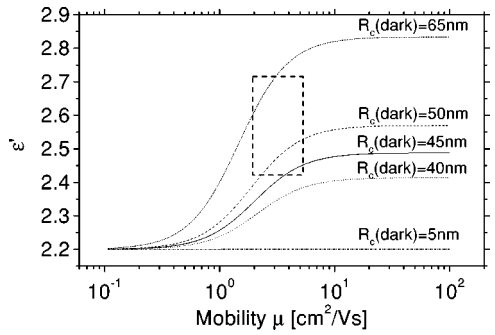

FIG. 5. The real part of the dielectric constant of porous GaP in the dark, calculated with the hydrodynamic model, is shown as a function of the mobility μ for different values of the radius R_c(dark). With an experimental value $\epsilon' = 2.57 \pm 0.15$ and a mobility μ between 1 and 5 $cm^2/V\,s$, we conclude that the radius R_c must be between 40 and 75 nm. (Only the lines that pass through the rectangle are compatible with the experimental values $\epsilon' = 2.57 \pm 0.15$ and $\Delta\epsilon'/\Delta\epsilon'' = 2.0 \pm 0.1$.)

of porous GaP in the dark, calculated with the hydrodynamic model, as a function of the mobility μ for different values of the radius R_c. From the fit of $\Delta\epsilon'/\Delta\epsilon''$ we know that the mobility μ is between 1 and 5 $cm^2/V\,s$. With an experimental value $\epsilon' = 2.57 \pm 0.15$ and a mobility μ between 1 and 5 $cm^2/V\,s$, we conclude that the radius R_c(dark) must be between 40 and 75 nm. In Fig. 6 we show the imaginary part of the dielectric constant of porous GaP in the dark, obtained with the hydrodynamic model, as a function of the mobility μ for different values of the radius R_c. With an experimental value $\epsilon'' = 0.07 \pm 0.05$ and a mobility μ between 1 and 5 $cm^2/V\,s$, we conclude that the radius R_c must be between 50 and 5 nm.

In summary we have shown that a combination of the results obtained from the fitting of $\Delta\epsilon'/\Delta\epsilon''$ and from the values of ϵ' and ϵ'' in the dark provides the mobility inside the semiconducting part of macroporous GaP $\mu = 3 \pm 1$ $cm^2/V\,s$ and the radius of the semiconducting part in the dark $R_c(\text{dark}) = 45 \pm 5$ nm.

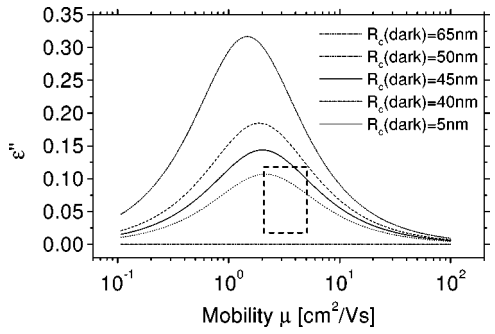

FIG. 6. The imaginary part of the dielectric constant of porous GaP in the dark, calculated with the hydrodynamic model, is shown as a function of the mobility μ for different values of the radius R_c. With an experimental value $\epsilon'' = 0.07 \pm 0.05$ and a mobility μ between 1 and 5 $cm^2/V\,s$, we conclude that the radius R_c must be between 50 and 0 nm. (Only the lines that pass through the rectangle are compatible with the experimental values $\epsilon'' = 0.07 \pm 0.05$ and $\Delta\epsilon'/\Delta\epsilon'' = 2.0 \pm 0.1$.)

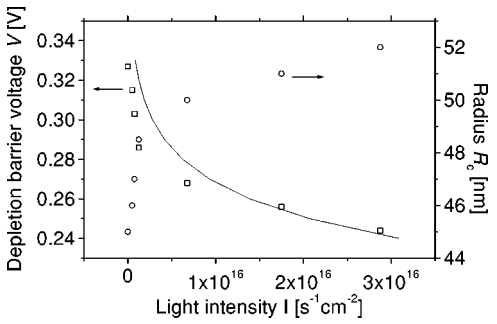

FIG. 7. The radius R_c of the semiconducting core (○) in the macroporous GaP matrix obtained from Fig. 3 and the potential difference across the depletion layer (□) surrounding the core, calculated with Eq. (1) is shown as a function of the incident ligh intensity. The experimental values for the potential are fitted with Eq. (3).

The value for the mobility μ inside the GaP particle is about a factor 40 smaller than that in bulk GaP obtained with Hall measurements;[27,28] $\mu = 130$ $cm^2/V\,s$. At present, the reason for this difference is not clear. We remark that the scattering of the electrons at the depletion barrier cannot account for the discrepancy, since the mean free path length of electrons in GaP is much smaller than the dimensions of the structures. Long-range transport through macroporous GaP was studied by light intensity modulated photocurrent spectroscopy.[13] The effective mobility ranged between 10^{-2} (at high light intensity) and $10^{-5} cm^2/V\,s$ (at low light intensity) and is thus 2–5 orders of magnitude smaller than the short-range mobility obtained by microwave reflectivity measurements with structural identical macroporous GaP. In addition, the mobility that we obtain is independent of the incident light intensity and thus of the position of the electron Fermi level in macroporous GaP. These contrasting results highlight the differences between long-range electron transport (with transport paths of 10–200 μm through the porous network) attenuated by multiple trapping/detrapping and short-range motion (transport path 1 nm) in the interior of the network far from surface localized traps.

Deri and Spoonhower[19] studied the photoinduced changes $\Delta\epsilon'$, and $\Delta\epsilon''$ upon illumination of a AgCl powder. They found that $\Delta\epsilon'$ and $\Delta\epsilon''$ were correlated, as in the case reported here. Very likely, the origin of $\Delta\epsilon'$, $\Delta\epsilon''$ is similar to that for GaP, i.e., an expansion of the semiconducting region inside the AgCl nanocrystals upon illumination.

ELECTRON-HOLE RECOMBINATION IN MACROPOROUS GAP

With the values for μ and R_c(dark) we can fit the changes in the complex dielectric constant under illumination by increasing the radius R_c (see Fig. 3). In Fig. 7 we plot the radius of the semiconducting part R_c as a function of the light intensity as obtained from the fit in Fig. 3. The electro*static* potential difference over the depletion layer V (which is four orders of magnitude larger than the microwave induced potential difference over the depletion layer) can be related to the width of the depletion layer $R - R_c$ via

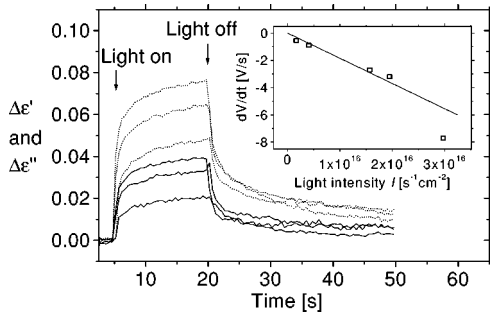

FIG. 8. The transients in the real part (dotted line) and the imaginary part (solid line) of the dielectric constant of porous GaP upon switching on and off the illumination for different light intensities ($I=1.25$, 3.8, and 12.5×10^{15} s^{-1} cm^{-2}). Insert: Rate of decay of the potential difference across the depletion layer dV/dt, measured a few ms after turning on the light, as a function of the incident light intensity.

$$V=\frac{e\,n}{3\epsilon\epsilon_0}\left(\frac{1}{2}R^2-\frac{3}{2}R_c^2+\frac{R_c^3}{R}\right), \tag{1}$$

where ϵ is the static dielectric constant of undoped GaP. The potential difference over the depletion layer is also shown in Fig. 7.

Figure 8 shows the transients $\Delta\epsilon'$ and $\Delta\epsilon''$ upon turning the illumination on and off. It is clear that $\Delta\epsilon'$ and $\Delta\epsilon''$ are correlated, i.e., show the same time dependence. This further supports our explanation on the basis of the hydrodynamic model. We remark that correlated $\Delta\epsilon'$ and $\Delta\epsilon''$ transients were also reported for polycrystalline CdS electrodes.[20] The ϵ transient is multiexponential, on a very slow time scale of seconds to minutes. This reflects that the photogenerated electrons have to overcome the energy barrier of the depletion layer before recombination at the surface is possible. The first milliseconds after switching on the illumination, the change in the potential is linear in time. In the inset, we have plotted the initial rate of change of the depletion layer dV/dt as a function of the light intensity I. The initial decay dV/dt is linear in I.

The increase in the radius of the semiconducting sphere R_c upon illumination is due to the photogeneration of excess free electrons. We explain the transients and the increase of R_c with I by a model that accounts for photogeneration in the bulk GaP and recombination at the surface and in the bulk.

Illumination with light with a photon energy $h\nu$ larger than the band gap (2.3 eV for GaP) generates electron-hole pairs. Since the absorption length α^{-1} for light with this photon energy ($\alpha^{-1}=2\times10^{-5}$ m) is much larger than the particle radius R, the creation of electron-hole pairs can be considered as uniform in a GaP sphere and the total rate of electron-hole pair generation in the particle equals $\frac{4}{3}\pi R^3\alpha I$, where I is the incident photon flux. Since the diffusion length for holes, $L_p=80$ nm,[31] is larger than the radius of the particle, every hole reaches the surface; this occurs on a time scale t_d which is given by the equation

$$R=\left(\frac{k_BT}{e}\mu_h t_d\right)^{1/2}, \tag{2}$$

where μ_h is the hole mobility. For our GaP particles this diffusion time t_d is 10^{-11} s, and thus much smaller than the time resolution of our measuring method. A fraction f_s of the holes becomes trapped in a surface state; the rest recombines in the bulk. Independent measurements of GaP single crystal electrodes (photoluminescence, electroluminescence and photocapacitance) showed that electrons and holes recombine in the bulk solid as well as the surface.[32] The change in the number of free electrons in a semiconducting particle per unit time under illumination thus becomes

$$\frac{dN}{dt}=-4\pi R^2 n\exp\frac{-eV}{kT}\beta_n S+\frac{4}{3}\pi R^3\alpha I f_s+\frac{4}{3}\pi R^3 g_{th}f_s\,. \tag{3}$$

The first term describes the trapping rate of free electrons in surface states. This rate is proportional to the number of free electrons at the surface $n\exp(-eV/kT)$, to the capture rate for free electrons in surface states β_n and the number of unoccupied surface states per unit surface area S. The second term describes the photogeneration of free electrons and the third term describes the thermal generation rate of free electrons.

The steady-state condition for Eq. (3) yields an expression for the depletion layer barrier V as a function of the light intensity I. The only unknown parameter in this expression is $\beta_n S/f_s$. Fitting the results presented in Fig. 7 with the expression for $V(I)$ [obtained from Eq. (3)], we obtain $\beta_n S/f_s=2\pm1$ cm/s^{-1}.

We now consider the time dependence of the potential difference over the depletion layer. Immediately after the illumination is switched on, the first and third terms on the right-hand side of Eq. (3) still counterbalance each other; the rate of change dN/dt of the number of free electrons in a GaP particle is completely determined by the photogeneration term (second term). For small variations in N we can develop the depletion layer voltage V around its value in the dark to obtain

$$\left.\frac{\Delta V}{\Delta t}\right|_{V\simeq V_{dark}}=\frac{\Delta V}{\Delta R_c}\frac{\Delta R_c}{\Delta N}\frac{\Delta N}{\Delta t}=\frac{\Delta V}{\Delta R_c}\frac{\Delta R_c}{\Delta N}\frac{4}{3}\pi R^3\alpha I f_s\,. \tag{4}$$

Thus the initial change in the depletion layer barrier per unit time is linear in the intensity of the illumination.

By fitting Eq. (4) to the experimental results (see the inset of Fig. 8) we obtain $f_s=0.5\pm0.1$. Combining this result with the value for $\beta_n S/f_s$ we obtain $\beta_n S=1\pm0.5$ cm/s. In order to estimate the capture rate constant β_n, we assume a reasonable density of surface states $S=10^{12}$ cm^{-2}. For this value of S we obtain an electron capture constant $\beta_n=10^{-12}$ cm^3/s. This value of the capture rate constant corresponds to a capture cross section $\beta_n/(\text{thermal velocity})\simeq10^{-20}$ cm^2, which is orders of magnitude smaller than the geometrical cross section of an atomiclike center (10^{-15} cm^2). Similar results for the electron-capture cross section have been reported for InP crystals, while GaAs crystals show even lower values for the electron-capture cross section.[33]

In summary, we have shown that the electron-hole pairs photogenerated in a porous GaP network recombine in the bulk as well as at the internal surface. The increase in the surface barrier for the photogenerated electrons forms the main reason for the increasingly slower electron-hole recombination rate after turning off photoexcitation.

APPENDIX A: DIELECTRIC CONSTANT OF A POROUS SEMICONDUCTOR

We discuss a model for the dielectric constant of porous GaP at microwave frequencies. During one microwave period $2\pi/\omega \simeq 10^{-10}$ s, free electrons are transported over a distance which is at maximum given by $\mu E 2\pi/\omega$, where E is the microwave-induced electric field inside the semiconducting part and μ is the mobility inside the semiconducting part. Due to screening, the electric field strength in the semiconducting part is smaller than the amplitude of the applied microwave electric field which is of the order of 10 V/cm. With the mobility μ for bulk GaP [$\mu = 130$ cm^2/V s (Refs. 27 and 28)] we obtain a transport distance of the order of 1 nm. This distance is much smaller than the size of the porous structure. The dielectric constant obtained from microwave conductivity measurements thus reflects the short-range motion of the free electrons in macroporous GaP. Figure 1 shows that the porous structure is random and has a typical size of 150 nm. Therefore, in a description of the dielectric constant of porous GaP at microwave frequencies, we can model the porous structure as a collection of isolated spheres with a typical radius R equal to 75 nm. Because of surface states with an energy level in the band gap, a region at the surface of the semiconductor is depleted of free electrons and only the inner core of these spheres, with a radius R_c is semiconducting.

In the Clausius-Mossotti approximation, the dielectric constant ϵ of a collection of particles is related to the polarizability of one particle α via[29]

$$\frac{\epsilon(\omega)-1}{\epsilon(\omega)+2} = f\alpha(\omega). \tag{A1}$$

In this expression f is the fraction of the volume of the spheres to the total volume. In a complex representation of physical quantities, the time dependence is given by $\exp(-i\omega t)$, and α and ϵ can become complex numbers. The modulus of α is proportional to the size of the induced dipole moment while the phase factor of α describes the delay of the induced dipole moment on the applied electric field. The polarizability of a mildly doped semiconducting sphere was discussed extensively in Ref. 21. There it was found that the electric field in the semiconducting part is screened over a distance equal to the Debye length L (see Fig. 2). In the less accurate Mie model, screening is completely localized at the surface. Therefore, the Mie model is valid only for particles in which the size is much larger than the Debye screening length L.

At the end of the Appendix we discuss the modifications to Ref. 21 needed to account for the presence of a depletion layer around the semiconducting sphere. Parameters in the expression for the polarizability α of a weakly conducting sphere surrounded by a nonconducting dielectric shell [Eq. (B6)] are the outer radius R and the dielectric constant ϵ of the dielectric background in which the free electrons move. We estimate R to be 75 nm from SEM images (see Fig. 1), and from the literature we take ϵ to be 8.5.[30] With an effective electron mass $m_n = 0.35 m_e$, where m_e is the bare electron mass,[30] and a free electron density n equal to the doping density ($= 3\times 10^{17}$ cm^{-3}) the other parameters of α become $L = \sqrt{\epsilon\epsilon_0 kT/ne^2} = 6.4$ nm and the plasma frequency $\Omega_p = \sqrt{ne^2/\epsilon\epsilon_0 m_n} = 1.8\times 10^{13}$ Hz. The only parameters not determined yet by an independent measuring method are the radius of the semiconducting part in the dark R_c(dark), under illumination $R_c(I)$ and the mobility of the free electrons inside the semiconducting core.

APPENDIX B: EXPLICIT CALCULATION OF THE POLARIZABILITY α OF A WEAKLY CONDUCTING SPHERE SURROUNDED BY A DIELECTRIC SPHERE

For wavelengths long compared to the size of a particle, the applied field **E** can be considered uniform on the scale of the particle. We assume the electric field to be directed along the z axis. For this case the electrostatic potential outside of the sphere has the form (in spherical coordinates)

$$\Phi_o(r,\theta) = \left(-Er + \frac{1}{4\pi\epsilon_0}\frac{p}{r^2}\right) P_1(\cos\theta), \tag{B1}$$

where the second term is the polarization field caused by the dipole moment p induced in the sphere. Note that the polarizability of the particle $\alpha(\omega)$ is related to the dipole moment $p(\omega)$ via

$$p(\omega) = 4\pi R^3 \epsilon_0 \alpha(\omega) E(\omega). \tag{B2}$$

Inside the conducting sphere the potential has the form

$$\Phi_c(r,\theta) = \left[aB\left(\frac{r}{\zeta}\right) + br\right] P_1(\cos\theta), \tag{B3}$$

where B is a spherical Bessel functions of the first kind and ζ is the complex Helmholtz length (see Ref. 21). Inside the depletion layer the potential obeys the Laplace equation, and has the form

$$\Phi_d = \left(\frac{c}{r^2} + dr\right) P_1(\cos\theta). \tag{B4}$$

The five unknowns a,b,c,d, and p are determined from the boundary conditions at the conducting and depleted region interface and the depleted region and air interface.

At the conducting and depleted region interface we require (i) $\Phi_c(R_c) = \Phi_d(R_c)$, and (ii) $\epsilon_c(\partial/\partial r)\Phi_c(R_c) = \epsilon_d(\partial/\partial r)\Phi_d(R_c)$ (the continuity of the component of D perpendicular to the interface) and (iii) $\partial/\partial r(\Phi_c - L^2\triangle\Phi_d)|_{r=R_c} = 0$ (the electron flow tangential to the interface), where $\epsilon_c(\epsilon_d)$ is the dielectric constant of the dielectric backgound in which the electrons move in the conducting

(depleted) region. At the depleted region and air interface we require (iv) $\Phi_d(R)=\Phi_o(R)$ and (v) $\epsilon_d \partial/\partial r \Phi_d(R) = \partial/\partial r \Phi_o(R)$ (the continuity of the component of D perpendicular to the interface).

By solving these five equations we obtain the expression for the polarizability

$$\alpha = 1 - \eta\chi R^3 - R_c^3\chi. \tag{B5}$$

In this expression,

$$\eta = \frac{R_c B'(1-\delta) + 2\dfrac{\epsilon_d}{\epsilon_c}(B\zeta - B'\delta R)}{\dfrac{\epsilon_d}{\epsilon_c}(B\zeta - B'\delta R) - R_c B'(1-\delta)} \tag{B6}$$

$$\delta = 1 - \frac{L^2}{\zeta^2} \tag{B7}$$

and

$$\chi = \frac{3}{2R_c^3(1-\epsilon_d) + \eta R^3(\epsilon_d + 2)}. \tag{B8}$$

The validity of this expression is verified for two special cases.

(i) For a semiconducting sphere without dielectric shell,

$$\lim_{R\to R_c} \alpha = \frac{[\epsilon_c - \delta(\epsilon_c - 1)]\dfrac{R}{\zeta}B' - B}{[\epsilon_c - \delta(\epsilon_c + 2)]\dfrac{R}{\zeta}B' + 2B}, \tag{B9}$$

which is the expression derived in Ref. 21.

(ii) For a nonconducting sphere (with $\epsilon_c = \epsilon_d$),

$$\lim_{L\to\infty} \alpha = \frac{\epsilon_c - 1}{\epsilon_c + 2}, \tag{B10}$$

which is the well-known expression for the polarizability of a dielectric sphere.

[1] J.J. Kelly and D. Vanmaekelbergh, Electrochim. Acta **43**, 2773 (1998).
[2] B. O'Regan and M. Gratzel, Nature (London) **353**, 737 (1991).
[3] U. Bach, D. Lupo, P. Comte, J. Moser, F. Weissortel, J. Salbeck, H. Spreitzer, and M. Gratzel, Nature (London) **395**, 583 (1998).
[4] M. Gratzel, Nature (London) **409**, 575 (2001).
[5] D. Cummins, G. Boschloo, M. Ryan, D. Corr, S. Nagaraja Rao, and D. Fitzmaurice, J. Phys. Chem. B **104**, 11 449 (2000).
[6] H. Weller, Adv. Mater. **5**, 88 (1993).
[7] F. Cao, G. Oskam, and P.C. Searson, J. Phys. Chem. **100**, 17 021 (1996).
[8] P.E. de Jongh and D. Vanmaekelbergh, Phys. Rev. Lett. **77**, 3427 (1996).
[9] P.E. de Jongh and D. Vanmaekelbergh, J. Phys. Chem. B **101**, 2716 (1997).
[10] P.E. De Jongh, E.A. Meulenkamp, and D. Vanmaekelbergh, J. Kelly, J. Phys. Chem. B **104**, 7686 (2000).
[11] L. Dloczik, O. Ileperuma, I. Lauermann, L. Peter, E. Ponomarev, G. Redmond, N. Shaw, and I. Uhlendorf, J. Phys. Chem. B **101**, 10 281 (1997).
[12] E.A. Meulenkamp, J. Phys. Chem. B **103**, 7831 (1999).
[13] A.L. Roest, P.E. de Jongh, and D. Vanmaekelbergh, Phys. Rev. B **62**, 16 926 (2000).
[14] D. Vanmaekelbergh, F. Iranzo- Marin, and J. van de Lagemaat, Ber. Bunsenges. Phys. Chem. **100**, 616 (1996).
[15] R. Konenkamp, Phys. Rev. B **61**, 11 057 (2000).
[16] H. Scher, M.F. Shlesinger, and J.T. Bendler, Phys. Today **44**, 26 (1991).
[17] D. Vanmaekelbergh and P.E. de Jongh, Phys. Rev. B **61**, 4699 (2000).
[18] J. van de Lagemaat and A.J. Frank, J. Phys. Chem. B **104**, 4292 (2000).
[19] R.J. Deri and J.P. Spoonhower, Phys. Rev. B **25**, 2821 (1982).
[20] S.Y. Grabtchak and M. Cocivera, Phys. Rev. B **50**, 18 219 (1994).
[21] E. van Faassen, Phys. Rev. B **58**, 15 729 (1998).
[22] D. Vanmaekelbergh, B. Erné, C. Cheung, and R. Tjerkstra, Electrochim. Acta **40**, 689 (1995).
[23] F. Schuurmans, D. Vanmaekelbergh, J. van de Lagemaat, A. Lagendijk, Science **284**, 5411 (1999).
[24] B. Erné, D. Vanmaekelbergh, and J. Kelly, J. Electrochem. Soc. **143**, 305 (1996).
[25] M. Sucher and J. Fox, *Handbook of Microwave Measurements* (Polytechnic, New York, 1963).
[26] N. Marcuvitz, *Waveguide Handbook 10* (McGraw-Hill, New York, 1951).
[27] M. Sotoodeh, A. Khalid, and A. Rezazadeh, J. Appl. Phys. **87**, 2890 (2000).
[28] Y. Kao and O. Eknoyan, J. Appl. Phys. **54**, 2468 (1983).
[29] J. Jackson, *Classical Electrodynamics* (Wiley, New York, 1998).
[30] S. J. Fonash, *Solar Cell Device Physics* (Academic, New York, 1981).
[31] B. Erne, D. Vanmaekelbergh, and J. Kelly, Adv. Mater. **7**, 739 (1995).
[32] D. Vanmaekelbergh, R. ter Heide, and W. Kruijt, Ber. Bunsenges. Phys. Chem. **93**, 1103 (1989).
[33] R. Bube and F. Cardon, J. Appl. Phys. **35**, 2712 (1964).